Health burden from food systems is highly unequal across income groups

Lianming Zheng[1,2], Wulahati Adalibieke[3], Feng Zhou[3,4,*], Pan He[5,*], Yilin Chen[1,2,6], Peng Guo[1,2], Jinling He[1,2], Yuanzheng Zhang[3], Peng Xu[7], Chen Wang[1,2], Jianhuai Ye[1,2], Lei Zhu[1,2], Guofeng Shen[3], Tzung-May Fu[1,2], Xin Yang[1,2], Shunliu Zhao[8], Amir Hakami[8], Armistead G. Russell[9], Shu Tao[1,2,3], Jing Meng[10,*], Huizhong Shen[1,2,*]

[1]Shenzhen Key Laboratory of Precision Measurement and Early Warning Technology for Urban Environmental Health Risks, School of Environmental Science and Engineering, Southern University of Science and Technology, Shenzhen, Guangdong, China

[2]Guangdong Provincial Observation and Research Station for Coastal Atmosphere and Climate of the Greater Bay Area, Southern University of Science and Technology, Shenzhen, Guangdong, China

[3]Institute of Carbon Neutrality, Laboratory for Earth Surface Processes, College of Urban and Environmental Sciences, Peking University, Beijing, China

[4]College of Geography and Remote Sensing, Hohai University, Nanjing, Jiangsu, China

[5]School of Earth and Environmental Sciences, Cardiff University, Cardiff, Wales, United Kingdom

[6]School of Urban Planning and Design, Peking University, Shenzhen Graduate School, Shenzhen, Guangdong, China

[7]Institute of Surface-Earth System Science, School of Earth System Science, Tianjin University, Tianjin, China

[8]Department of Civil and Environmental Engineering, Carleton University, Ottawa, ON, Canada

[9]School of Civil and Environmental Engineering, Georgia Institute of Technology, Atlanta, Georgia, United States

[10]The Bartlett School of Sustainable Construction, University College London, London, United Kingdom

*Corresponding author, e-mail: zhouf@pku.edu.cn; hep3@cardiff.ac.uk; jing.j.meng@ucl.ac.uk; shenhz@sustech.edu.cn

Abstract

Food consumption contributes to the degradation of air quality in regions where food is produced, creating a contrast between the health burden caused by a specific population through its food consumption and that faced by this same population as a consequence of food production activities. Herein, we explore this inequality within China's food system by linking air pollution–related health burden from production to consumption, at high levels of spatial and sectorial granularity. We find that low-income groups bear a 70% higher air pollution-related health burden from the food production than is caused by their food consumption, while high-income groups benefit from a 29% lower health burden relative to their food consumption. This discrepancy largely stems from a concentration of low-income residents in food production areas, exposed to higher emissions from agriculture. Comprehensive interventions targeting both production and consumption sides can effectively reduce health damages and concurrently mitigate associated inequalities, while singular interventions exhibit limited efficacy.

Introduction

Agricultural intensification and redistribution have significantly increased food productivity and the abundant and diverse food supply[1,2]. However, these practices have also resulted in an uneven distribution of the environmental footprint of the food system. Emissions embedded in the food system are spread across various food-producing regions that may be far from where the food is consumed. Globally, 26%–64% of the population cannot fulfill their crop demand solely through crop production within a 1000-km radius[3]. In China, Henan, Hebei, and Shandong provinces accounted for about one-third of agricultural ammonia (NH_3) emissions[4], while local food consumption only constituted 11%–19% of the national food consumption[5]. Consequently, food contributes one of the greatest disparities in consumption-based $PM_{2.5}$ (fine particulate matter with diameter <2.5 μm) pollution exposure among all goods[6], potentially leading to significant environmental inequality among different groups of people. In the United States, non-Hispanic whites exhibit higher food consumption rates and consequently cause a 61% greater air pollution exposure compared to their black and Hispanic counterparts[6].

In alignment with the United Nations Sustainable Development Goals, the modern food system needs to feed the global population to provide nutritional security with low environmental impact and without contributing to social injustice[7-13]. To avoid a disproportionate allocation of health

outcomes to a small subset of the population, a key step is to explicitly evaluate the inequality of the health damage attributed to the food system, which is rarely discussed. Key factors such as food categories, spatial heterogeneity, and potential drivers (e.g., household wealth) have not been adequately explored, impeding efforts to reduce inequality. Taking food categories as an example, ruminant meat, especially beef, has the highest environmental impact compared to non-ruminant meat, whereas plant-based foods have the least impact[14,15]. However, the manner and degree to which food categories affect general health-related inequalities remain unknown, and it is unclear whether existing intervention strategies aimed at alleviating environmental burdens and mitigating the negative health effects of the food system can provide co-benefits in reducing related inequalities.

Expanding on this concept, we examine the air pollution–related inequality within China's food system. As the world's leading agricultural producer, China has experienced significant agricultural intensification[16]. This transformation is partially driven by the nutritional requirements of its sizable population, exacerbated by the limited per-capita arable land compared to the global average[17]. The inherent contradiction arising from the restricted agricultural land and the escalating food demand has necessitated farmers to enhance their food production efficiency, thereby fueling the process of agricultural intensification. These factors and a diverse dietary transition[18] make China's food system an important case for understanding air pollution–related inequality.

Results

Spatial heterogeneity in air pollution–related health impact

We quantified air pollution–related health damage, represented by premature mortality, throughout the food supply chain. Our analytical framework integrates several components: a high-resolution emission inventory with 1 km × 1 km resolution for NH_3 emissions from cropland and livestock management, developed by Adalibieke et al.[19] and Wang et al.[20] as well as 10 km × 10 km resolution for NH_3 emissions from non-agricultural activities[21] and other pollutants (e.g., primary $PM_{2.5}$, SO_2, NO_x) from all sources[22-25], derived from the PKU Inventory for the baseline year 2017 (see Methods and Data); a provincial-level input–output table; and an advanced backward sensitivity analysis technique implemented within a regional chemical transport model (CMAQ-Adjoint)[26]. Using the adjoint model enabled us to trace air pollution–related health damage from

production to consumption across nine distinct food categories at a high level of spatial and sectoral granularity (Methods and Data). This fine resolution facilitated the investigation of air pollution–related inequality within the food system.

In general, the food system in China was responsible for approximately 0.26 (95% confidence interval (CI), [0.22, 0.32]) million premature deaths related to ambient $PM_{2.5}$ exposure in 2017. Most (74%) of these deaths are attributed to NH_3 emissions, an important precursor of ambient $PM_{2.5}$, during food production, such as crop cultivation and livestock breeding. The remainder (26%) are caused by emissions of primary PM and other precursors, including SO_2 from power plants and NO_x from motor vehicles, during the distribution, aggregation, processing, packaging, and marketing of food products. This food–induced air pollution-related mortality represents 12% of overall annual mortality from exposure to ambient $PM_{2.5}$ in China. Of this mortality, meat contributes 55%; grains contribute 30%; and vegetables, fruits, and non-meat animal products (including eggs and dairy) account for the remaining 15% (see Supplementary Text1 for a comparative analysis of our results and previous studies).

Northern and Eastern China are the regions most affected by food production (Fig. 1a and Supplementary Fig. 1a), and 41% of the mortality is attributable to food production (defined as "M_P") concentrated in Shandong, Henan, Hebei, and Jiangsu (Supplementary Fig. 1a). The spatial distribution is determined by regional population levels (Supplementary Fig. 2a) and agricultural NH_3 emissions (Supplementary Fig. 2b) in conjunction. The Gini coefficient, representing the inequality of spatial disparity for M_P, is estimated to be 0.31 on average and ranges from 0.30 to 0.64 by food type (Fig. 1d and Supplementary Fig. 3). The Gini coefficient of overall food in mortalities is relatively low compared to that of specific food types. This can be attributed to the evident spatial variation in the distribution of mortality rates caused by different food types (Supplementary Fig. 4), thereby mitigating the disparities in the spatial distribution of cumulative mortality rates.

The distribution of premature mortality rates based on food consumption ("M_C" rates) is more dispersed than that of M_P rates (Fig. 1b). The provinces with the highest air pollution–related mortality rates from their food consumption are Shanxi, Inner Mongolia, Shandong, Hubei, and Jiangsu. Two categories of regions emerged. The first category pertains to highly developed regions with wealthy populations, such as Beijing, Shanghai, Zhejiang, and Guangdong, which show higher

M_C rates than the others. The second category represents concentrated food-producing regions with developed agricultural production, such as Henan and Hebei, where M_C is far below M_P. The distribution of M_C is more closely associated with the spatial differences in population and regional dietary preferences, particularly in grains and meats consumption (Supplementary Fig. 5). The spatial inequality of M_C is significantly lower than that of M_P, with a Gini coefficient of 0.21 on average (ranging from 0.23 to 0.53 across different food types; Fig. 1d and Supplementary Fig. 3). Similar to M_P, the Gini coefficient of total mortality is lower, since the spatial heterogeneity of mortalities of different food type (Supplementary Fig. 6). The low inequality of M_C is attributed to a convergence toward a modernized diet (Supplementary Fig. 7) characterized by high meat consumption in the last few decades[5], which is consistent with global patterns[27,28].

Inequality by food categories

We calculated the difference between M_P and M_C rates, presented as ΔM rate in Fig. 1c (Methods and Data). Positive ΔM rates indicate that people in the region face a larger health burden from food production than that caused by food consumption ("production-oriented"), whereas negative ΔM rates signify the opposite ("consumption-oriented"). Overall, the ΔM rates vary geographically across the country. The consumption-oriented provinces include (1) regions with poor crop-growing conditions (e.g., Qinghai and Tibet) that face constraints with regard to food production and (2) highly developed regions (including provincial-level municipalities, such as Chongqing and Beijing, and coastal provinces, such as Zhejiang) where the industrial focus has shifted from agriculture to other industries[29]. Notably, the results of ΔM rates are strongly influenced by population size, as the considerably difference between the M_P and M_C rates in the total mortality would be scaled down owing to the high population in per-capita terms (e.g., Guangdong, as shown in Supplementary Fig. 1a, b) and vice versa (e.g., Tibet, Hainan, and Qinghai; Supplementary Fig. 1a, b).

Henan exhibited the highest positive ΔM rate, with 1.06 (95% CI: [0.00, 2.13]) premature deaths per 10,000 population. This region experiences severe food-induced air pollution, which locally causes 2.95 (95% CI: [0.93, 4.97]) premature deaths per 10,000 population. Comparatively, food consumption in Henan is responsible for 1.88 (95% CI: [0.91, 2.86]) premature deaths per 10,000 population nationwide. Thus, the population in Henan bears a 57% higher health burden due to food production than that caused by their food consumption. Conversely, Beijing exhibited the

lowest ΔM rate, with a value of −1.32 (95% CI, [−0.88, −1.77]; 0.74 (95% CI, [0.24, 1.25]) and 2.06 (95% CI, [1.59, 2.55]) for the M_P and M_C rates, respectively, and a 64% lower health burden). Given the limitations of existing inequality metrics, such as the Gini coefficient and the pollution inequity index proposed by Tessum et al.[6], in evaluating the inequality between production and consumption (i.e., ΔM rates with both positive and negative values), we developed a Supply–Demand Health Inequality Index (SDHII) to estimate national inequality in the ΔM rates. This index incorporates the discrepancy between the production- and consumption-based mortality rates of individual population groups and weights them by population size to get the final national-level inequality. As a result, this index evaluates the inequality compared with an ideal state of complete equality (Methods and Data; Supplementary Fig. 8) and to ensure the comparability of the inequality between specific sectors and food categories.

Grains, poultry, and pig meat were identified as the top three food types associated with the highest inequality, whereas vegetables, fruits, and non-meat animal-sourced foods (eggs and dairy) demonstrated minor inequality (Fig. 2 and Supplementary Table 1). The low level of inequality associated with vegetables and fruits can be attributed to their smaller environmental footprint, perishable nature, and difficulties in storage[30], thus tending to be consumed locally. When considering inequality across protein types, the disparity is considerably greater for animal-sourced protein than for plant-sourced protein, particularly for red meat (livestock meat, including beef, pig meat, sheep and goat) and poultry (Supplementary Fig. 9), resonates with findings from previous studies that assess the environmental footprint of food protein[18,31]. In highly developed and coastal provinces, the health cost of producing 1 kg of protein was significantly higher than the cost of consuming 1 kg of protein (e.g., 2–9 times higher in Beijing, Shanghai, and Tianjin compared with the current consumption cost; Supplementary Fig. 9, right end of the curves). The substantial health inequality of animal protein primarily stems from a higher air quality-related mortality per unit of animal protein consumed compared to that of plant protein (Supplementary Fig. 10).

We investigated the inequality of the food system between rural and urban areas (segmented by each province) and at different income groups. To explore income-related inequality, we classified the provinces into ten income groups based on per capita disposable income, denoted as D1 to D10 in descending order (i.e., D1 is the highest income group while D10 is the lowest; Supplementary Table 2; see Methods and Data). Pronounced gaps in ΔM rates exist between rural

and urban areas (Supplementary Fig. 11) due to the rural-urban differences in M_P and M_C rates (Supplementary Fig. 12), particularly for Inner Mongolia in sheep and goat since the focus production in rural area while high consumption in urban area (Supplementary Fig. 11). Depending on food type, 57%–94% of the rural population is exposed to higher health risks from production (Supplementary Table 3) than they should be according to their consumption, compared to only 0%–22% for their urban counterparts. Particularly for red meat, over 90% of the rural population bears an excess health burden, compared to 0%–16% for the urban population. This is primarily attributable to the substantially higher emissions exposed during production in rural areas compared to urban areas (Supplementary Fig. 13).

M_C rates increase with income (Fig. 3a). The highest mortality rate occurred in the second highest income group, D2 (2.45 deaths per 10,000 population; 95% CI, [1.59, 3.34]). However, a significant decline was observed in the top income group, D1 (1.43 deaths per 10,000 population; 95% CI, [1.41, 2.45]; Fig. 3a). This decline is attributed to the lowest contribution of meat consumption to per-capita deaths in D1 compared to other high-income groups (D2–D5), due to their health-conscious diet with lower grains and ruminant meat intake (Supplementary Table 4). In contrast, M_P are generally negatively correlated with income, although the lowest income groups (D9–D10) do not follow this trend due to harsh local conditions for crop growth (e.g., rural areas in Gansu, Qinghai, and Tibet). Overall, low-income groups (D6–D10) experienced 70% more health damage than high-income groups (D1–D5), but food consumption in the former caused 29% less health damage, leading to positive ΔM rates among low-income groups, negative ΔM rates among high-income groups, and net inequality over income, which is dominated by animal-based food (Fig. 3b). The ΔM rate of D5 is as low as that of the highest income groups D1–D2, mainly because these groups comprise urban areas in provinces with poor planting conditions (e.g., urban areas in Qinghai and Shanxi), resulting in the lowest M_P rate from grains among all income groups. The inherent cause of mortality rate inequality across income groups lies in the higher concentration of low-income individuals residing in regions of food production, exposing them to elevated NH_3 emissions. This phenomenon becomes evident when examining per capita emissions (Supplementary Fig. 14), where the low-income regions (D6–D10; 9.0 kg per capita) emits 2.6 times more NH_3 than the high-income group (D1–D5; 3.4 kg per capita). When attributed to food consumption, the contribution is relatively limited, with no significant difference observed in per

capita emissions between low-income (5.8 kg per capita) and high-income (6.1 kg per capita) groups.

To trace the sources of inequality caused by food supply between income groups, we calculated net ΔM by deducting the portion that achieved a balance between mutual trade across specified income groups (Methods and Data). Net ΔM represents the total number of net premature deaths, i.e., the overall number of premature deaths caused by one income group to another income group, after subtracting the equivalent premature deaths induced by mutual food supply. The connection between income and net ΔM was evident (Fig. 4a). Generally, higher income groups (D1–D5) exhibit fewer net ΔM because of their limited food exports to lower income groups (D6–D10), whereas the lower income groups bear greater health damage from supplying food to higher income groups. Notably, D6–D8 suffered more from food supply (positive net ΔM) than the D7–D10 groups (Fig. 4a, upper left), while net less health cost (negative net ΔM) is observed in D1–D4 (Fig. 4a, lower right). Similar results were observed across all food types (Fig. 4b), indicating that high-income groups transfer the environmental externalities through interregional food trades, while low-income groups bear excess health damage, regardless of food type. The grains exhibit a greater proportion of net ΔM in the D8 group attributed to other income groups, suggesting that D8 bears a greater burden of premature mortality from the production of grains that is consumed by other income group. This trend is primarily attributed to the prevalence of major agricultural provinces within the D8 income group, notably Henan, Hebei, Jilin, and Anhui (Supplementary Table 2). These provinces contributed prominently to national grain production (Supplementary Fig. 15b) and related NH_3 emission (Supplementary Fig. 15a), yet their consumption levels fall short of their production capacities (Supplementary Fig. 15c) due to local dietary preferences (Supplementary Fig. 15e) and population variance (Supplementary Fig. 15d). A substantial portion of grains from these provinces is transported to other regions for consumption, resulting in a noticeable net ΔM. By comparing premature mortalities resulting from self-production and consumption and interregional food trade, we found that the proportion of self-production and consumption increased with income (Supplementary Fig. 16 and 17). This suggests that agricultural products in developed regions are primarily produced to meet local demand rather than being traded on the national market for revenue. Considering all end-use sectors, we found that food contributes 41.7% of the total inequality of all end-uses in China (Supplementary Fig. 18 and

Supplementary Table 5), being the largest among all goods and services.

Intervention strategies to improve equality

Based on production- (emission mitigation) and consumption-based (diet transition) scenarios (Table 1), we combined and conducted 35 scenario simulations (Supplementary Table 6) to investigate whether individual scenarios or their combinations designed to reduce environmental pressure and health damage would yield synergistic benefits in reducing inequality.

Exclusively adopting production-based emission mitigation scenarios (with dietary patterns unchanged) leads to a noticeable improvement in both health damage and inequality, reducing SDHII by 22–35% and premature mortality by 20–44% (Fig. 5). The reduction in inequality among all production-based mitigation interventions primarily stems from decreased inequality within grain production (Supplementary Fig. 19).

The diet transition approaches (with production emission unchanged) exhibit considerable variability in inequality change (ranging from −30% to +18%; Fig. 5). Scenario DT3 (minimal adjustments of the current diet toward the recommended range) demonstrates a 30% decrease in inequality, whereas the DT4 scenario (consuming the average of the recommended range) exhibits a limited effect (6% reduction). This implies that the former is the most favorable dietary option, as it is the most practical choice for policy measures involving the minimal required transition in diets. The key reason for the limited effectiveness of certain dietary transition schemes (e.g., DT1 with maximal adjustment to the current diet) is that while reducing meat consumption contributes the most to improving equality, the benefits are offset by consuming plant-based foods (such as grains, vegetables, and fruits) and non-meat animal-based foods (including dairy and eggs; Supplementary Fig. 20).

In the combined approach of emission mitigation and dietary transition, there is a marked reduction in premature mortality and associated inequalities (denoted as SDHII). The adoption of moderate (DT3) and stringent (DT4) dietary transitions, alongside emission reduction strategies (EM1–EM6), leads to a further 12%–27% reduction in SDHII compared to individual EM1–EM6 measures and a concurrently decrease in mortality rates by 3–13%. Notably, the strictest production (EM6) and dietary (DT4) scenarios yield the most favorable results, reducing mortalities and SDHII by 55% and 62%, respectively. This underscores the synergistic potential of dual interventions at production and consumption sides in enhancing health damage reduction and

equality in the food system. Moreover, most scenarios modestly alleviate the uneven distribution of populations experiencing disproportionate health damage (Supplementary Table 7).

For the food production reallocation scenarios, although the premature mortalities decrease with increasing reallocation degrees (Supplementary Fig. 21), inequality (SDHII) and the proportion of the population experiencing disproportionate health damage increases slightly (Supplementary Table 8 and Supplementary Fig. 22). This suggest that agricultural reallocation aimed at reducing health damage is insufficient for alleviating inequality.

In addition to supply and demand-side interventions, economic policies such as taxation and subsidies can complement efforts to reduce inequality. By evaluating the value of a statistical life[33] (Supplementary Text2), we quantified the appropriate food tax that should be implemented or subsidy that should be provided in each region (Supplementary Fig. 23) and income group (Supplementary Fig. 24). Our findings indicate that middle- to high-income groups (D1–D5) should be subject to a 4%–14% food tax to compensate for the excess damage suffered by low- to middle-income groups (D6–D10), which could cover 6%–138% of the latter's food costs.

Discussion

Revealing the inequalities of health damage within the food system is crucial for understanding environmental justice and achieving the United Nations Sustainable Development Goal of reducing inequalities[34]. Our findings contribute to the ongoing discussion about the health effects of food systems, focusing on the equality of air-related health impacts. By linking food production and consumption, we highlight the disparities and inequalities between supply and demand ends across space and food types. Our findings uncover significant and disproportionate differences in air pollution–related health damage per-capita. Higher geographical inequality in production than consumption is observed, perhaps due to increasing agricultural intensification and resulting differences in provincial agricultural emissions. Another possible reason for the smaller demand-side inequality is the convergence toward regional diets over time, possibly due to the Chinese government's efforts to promote and guide healthy diets and improve living standards[35].

Our work provides a spatially resolved, food-specific analysis of health-effect inequalities within the food system. We identified optimal schemes to simultaneously reduce health damage and associated inequality, expanding the options available for developing and implementing dedicated mitigation policies. Nevertheless, substantial obstacles and challenges need to be addressed. For

example, while appropriate interventions can synergistically reduce health damage and inequality on a national scale (Fig. 5), a trend of mortality may not consistently align with that of equality when adopting certain more sustainable interventions (e.g., food production reallocation), particularly on a regional scale (e.g., the regions indicated at both ends of the curve in Supplementary Fig. 11 and 22). With the expected increase in agricultural intensification, concentrating food production in certain regions could widen the differential burdens of negative externalities of food production among regions and populations. Identifying the leverage points that balance agricultural yield, emission reduction, and equitable distribution of pollution burdens presents a complex problem for policymakers. Another emerging challenge for policymakers is the need for meticulous consideration of the growing importance of NH_3 in air pollution in the future. Stringent controls on NO_x and SO_2 may amplify NH_3's role in the formation of secondary aerosols[36,37], potentially resulting in greater health impacts. Furthermore, implementing diversified regulations and protocols to reduce inequality can be challenging. Our results show that food consumption recommendations (e.g., self-production and marketing, or import from other regions; food intake) may need to vary based on regional specifics, which could hinder the development and adoption of policy-related measures, especially when coordination between national and local policies is critical. Given the intricacy of food system transformation, policymakers must concurrently develop short- and long-term policies to address future challenges. In the short term, achieving a more equitable distribution of negative externalities in the food system may not be immediately feasible, so economic measures are recommended to compensate for excess health damage, such as implementing food taxes to subsidize food production regions (Supplementary Fig. 23 and 24). In the long term, policymakers need to phase in top-level design and restrictive policies for food system emissions and the related equality, accounting for factors such as the spatial heterogeneity of health costs associated with food production, anticipated dietary transitions in the local context, and nutritional requirements due to population growth, as well as the overall sustainability goals pursued by the nation. Our research investigates the potential synergies between health damage and inequalities (Fig. 5), providing valuable references for policy development.

As the world's most populous country, China faces tremendous pressure on its food supply system due to improved living standards. While the development of agricultural intensification and mature

food supply chains has satisfied the food demands, they have also led to significant food system-related inequalities. It is worth noting that China is not alone in experiencing these inequalities. In a follow-up first-order analysis that expands the current assessment scale, we found that countries worldwide, particularly middle- and high-income countries, exhibit significant inequality in agricultural NH_3 emissions exposure (Supplementary Text3, Supplementary Fig. 25). This observation indicates that countries with more advanced food systems may encounter greater challenges relating to agricultural emissions and associated inequalities. Our study illuminates the issue of food system inequality, offers valuable guidance for policymakers in China while also serves as a point of reference for the sustainable development of food systems worldwide.

Methods

We developed a comprehensive modeling framework to estimate the health damage due to $PM_{2.5}$ pollution exposure from the food system in China and analyzed the associated health damage inequality (Supplementary Fig. 26). The development of the framework includes several steps. Initially, the atmospheric emissions from the supply and demand sides of the food system were linked using the Multi-Regional Input–Output (MRIO) model[38]. Then, we used the Global Exposure Mortality Model (GEMM)[39] to estimate premature mortality associated with ambient $PM_{2.5}$ exposure and the sensitivities of premature mortality to ambient $PM_{2.5}$ concentrations by grid cell. Subsequently, we coupled the concentration sensitivities into multiphase Adjoint for the Community Multiscale Air Quality (CMAQ-Adjoint) model[26] to compute the sensitivities of premature mortality to emissions. These matrices encompass all pollutant species, locations, and time, allowing us to estimate their relative contributions on both the supply and demand sides. To analyze inequality, we developed an index, SDHII, to quantify the national inequality pattern in the gap between $PM_{2.5}$-related premature mortality associated with food supply and demand. The detailed procedures are described in the following sections.

Atmospheric emissions from food production to consumption

We initiated our study by developing a production-based emission inventory of all the production sectors of China in 2017, for which the global high-resolution emission inventory product (10 km × 10 km) published by Peking University (PKU-Inventory) for atmospheric emissions across sectors (e.g., power generation, industry, transportation, and agriculture), fuel types (e.g., coal, oil, natural gas, and biomass), and pollutants (e.g., primary $PM_{2.5}$, SO_2, NO_x, CO, OC, BC) was used[22-25]. Note

that PKU-Inventory also includes NH_3 emissions from non-agricultural activities[21]. Additionally, a Chinese agricultural emission inventory with 1 km × 1 km resolution developed by Adalibieke et al.[19] (crop NH_3 volatilization) and Wang et al.[20] (livestock management) was employed to calculate the NH_3 emissions associated with agricultural activities. This comprehensive inventory covered NH_3 emissions from the production of nine food categories, including grains, vegetables, fruits, pig meat, beef, sheep and goat, poultry, dairy, and eggs. The emissions from dairy and egg products considered in this study arise from the rearing processes of dairy cows and egg-laying hens. Due to a portion of grains being used for animal feed, we reallocated the NH_3 emissions from this feed portion to animal-sourced food. Using food consumption data of China extracted from the United Nations FAOSTAT database[40], we computed that in 2017, approximately 32% of grains was used for livestock feed in China. This proportion closely resembles the results of Liu et al., 2021 (34% in 2010)[41]. Subsequently, we redistributed the emissions from this portion of grains based on the NH_3 emission proportions of different animal-based food sources. By integrating this food emission inventory into the PKU-Inventory, we expanded the current inventory to provide a detailed account of agricultural emissions. Subsequently, we reallocated all the atmospheric pollutants according to provinces to align them with the production sectors in the MRIO models using Energy Balance Sheets from the China Energy Statistical Yearbook[42]. The resulting provincial production-based emission inventory comprised 42 production sectors (Supplementary Table 9) corresponding to the MRIO production sectors of the nine food categories.

To establish a link between pollutant emissions between the food supply and demand sides, we employed Environmental Extended Input–Output Analysis (EEIOA) to create a consumption-based emission inventory. EEIOA is an extended application of input–output analysis that enables the explicit analysis of environmental impacts[43]. Initially, we employed traditional economic accounting, expressing the input–output link function as Eq. (1):

$$X = (I - A)^{-1}Y \quad (1),$$

where X represents the economic output matrix, A is a normalized matrix of intermediate coefficients where columns correspond to the input required from sectors in a given region to produce one unit of the output of each sector in another region, $(I - A)^{-1}$ is the Leontief inverse matrix, and Y is a vector of the finished consumption. Subsequently, we incorporated emission information using Eq. (2):

$$E = f(I - A)^{-1}Y \quad (2),$$

where E represents atmospheric emissions embedded in flows of goods and services between the sectors. The matrix f is diagonal, with emission intensities (emissions for unit output) for each sector along the diagonal and zeros in all the other positions.

A consumption-based emission inventory (referred to as S) was generated using EEIOA that illustrates how emissions are embodied in the flows of goods and services among the production sectors, ultimately reaching the final consumption sectors. This inventory includes 31 provincial-level administrative divisions (excluding Taiwan, Hong Kong, and Macao, as data for these regions were unavailable), 42 production sectors, and 5 consumption sectors.

The consumption-based emission inventory quantifies virtual emission flows specific to each region, spanning from supply to demand sides. Subsequently, we calculated the emissions attributed to production (E_p) and consumption (E_c) at the provincial level using Eq. (3) and (4):

$$E_p = \sum_c S \quad (3)$$

$$E_c = \sum_p S \quad (4),$$

where S represents the consumption-based inventory; p and c is the supply and demand sides of the inventory, respectively; E_p is a transposed matrix of $\begin{pmatrix} E_p^1 & E_p^2 & E_p^3 & \cdots & E_p^Q \end{pmatrix}$, where E_p^i represents the production-based emissions in a given province i, and Q is the total number of administrative divisions (31 in this study, excluding Hong Kong, Macao, and Taiwan due to data limitations). Similarly, E_c is a transposed matrix of $\begin{pmatrix} E_c^1 & E_c^2 & E_c^3 & \cdots & E_c^Q \end{pmatrix}$, where E_c^i denotes the consumption-based emissions in a given province i.

Next, we computed the relative contribution of emissions for each province at both the supply and demand ends, denoted as:

$$r_{i,j} = \frac{S_{i,j}}{\sum_{c=1}^{Q} S_{i,c}} \quad (5),$$

where $r_{i,j}$ represents the relative share of emissions within a given region i at the supply side, concerning region j at the consumption end. To consolidate all relative shares of emissions along the supply chain, we employed the matrix R, defined as:

$$R = \begin{pmatrix} r_{1,1} & \cdots & r_{1,Q} \\ \vdots & \ddots & \vdots \\ r_{Q,1} & \cdots & r_{Q,Q} \end{pmatrix} \quad (6),$$

where R incorporates all the relative shares of emissions.

To appropriately allocate agricultural emissions within the food supply chain, we applied a double constraint to this portion of the emissions. First, we extracted the economic flow from the agricultural sectors to the rural and urban consumption sectors, as generated by the MRIO model. Next, we redistributed the food emissions of each province by (1) calculating the relative share of monetary flows from each province on the demand side to provinces on the demand side, yielding a supply-side constraint matrix (labeled as H_1); (2) determining the total amount of annual per-capita food consumption in 2017 for each food type using data from the Chinese National Bureau of Statistics[5]; and (3) matching the total food consumption to that of each province in the demand side and redistributing it according to H_1. These steps ensured that the relative proportions of each food type in the supply side for a given province were adequately constrained. Each food type was individually distributed on the demand side based on the scaling factors.

To ensure that the total amount of emissions was conserved for each food type from the supply to demand side, we calculated the relative share of the amount of food in the aforementioned result for each province on the supply side as an emission-constraint matrix (labeled as H_2). Subsequently, we redistributed agricultural emissions from the supply side to the demand side using H_2. Notably, we did not conduct a detailed analysis of the residential sectors because the overall estimation framework is based on the reclassification of the production sectors. Nevertheless, we treated this part as a whole and accounted for it when evaluating the contribution of each component to the premature mortality[44].

Health damage estimation

The latest version of the CMAQ-Adjoint, version 5.0, was utilized in our study to quantify the contributions of location-, time-, and pollutant-specific emissions to premature mortality. CMAQ-Adjoint is comprised of two models: a forward model, which mirrors the original CMAQ base model, and a backward model. We applied CMAQ-Adjoint to a geographical domain encompassing East Asia, defined by 124 × 184 horizontal grid cells at a resolution of 36 km, and 13 vertical layers extending to approximately 16 km above ground. For evaluation, a 1-year simulation using the CMAQ base model was conducted. The results have been illustrated in a previous study, indicating a general concordance with observed spatial distributions and temporal trends of multiple pollutants.

The backward model allowed us to calculate sensitivities, that is, the partial derivatives of the

objective function concerning related input parameters. By defining the objective function J as the total premature mortality from ambient $PM_{2.5}$ exposure within China in 2017, we incorporated the GEMM into the adjoint analysis. The objective function J was expressed by the following equations,

$$J = \sum M_{0,x,y} P_{x,y} \left[1 - e^{-\theta T(z_{x,y})}\right] \quad (7)$$

$$T\left(z_{x,y}\right) = \frac{\log\left(1+\frac{z_{x,y}}{\alpha}\right)}{1+e^{\frac{-(z_{x,y}-\mu)}{\nu}}} \quad (8)$$

$$z_{x,y} = max(0, C_{x,y} - cf) \quad (9)$$

where (*x*, *y*) denotes a specific model grid cell; $M_{0,x,y}$ represents the baseline mortality rate at grid cell (*x*, *y*); $P_{x,y}$ represents the population within grid cell (*x*, *y*); $C_{x,y}$ denotes the location-specific annual $PM_{2.5}$ concentration at grid cell (*x*, *y*), in μg·m^{-3}; *cf* is the concentration threshold below which no health association is assumed to be identifiable. The term $1 - e^{-\theta T}(z)$ is the GEMM equation to calculate the population-attributable fraction (PAF)[39]. As suggested by Burnett et al.[39], the following values for the GEMM parameters were used to calculate PAF of noncommunicable diseases and lower respiratory infections (NCD+LRI) mortality from ambient $PM_{2.5}$ exposure for adults aged 25–99: θ = 0.1430, α = 1.6, μ = 15.5, ν = 36.8, *cf* = 2.4 μg·m^{-3}. $M_{(x,y)}$ is determined by the baseline mortality rate of NCDs+LRIs of the province where (*x*, *y*) is located[45]. Further details regarding the parameter configuration of GEMM can be found elsewhere[39].

We then derived the adjoint forcing term using Eq. (10),

$$\varphi_{x,y} = \frac{\partial J}{\partial c_{x,y}} = M_{0,x,y} P_{x,y} \theta e^{-\theta T(z_{x,y})} T'(z_{x,y}) \frac{dz_{x,y}}{dc_{x,y}} \quad (10)$$

where $\varphi_{x,y}$ is the adjoint forcing at grid cell (*x*, *y*); $c_{x,y}$ denotes the $PM_{2.5}$ concentration at grid cell (*x*, *y*) at any time step; $dz_{x,y}/dc_{x,y}$ is equal to the reciprocal of the number of model time steps in a year and is set to 1/43800 in our simulation (12 minutes per time step); $T'(z_{x,y})$ is the derivative of $T(z)$ at $z = z_{x,y}$. In the adjoint simulation, these forcing terms were applied to all modeled $PM_{2.5}$ species as inputs to derive the adjoint sensitivities of mortality to location- and time-specific emissions of primary $PM_{2.5}$ and precursors. Similar assessment has been conducted in our CMAQ-adjoint development paper[26]. It should be noted that the computational expense of running the CMAQ-Adjoint model is about fourteenfold compared to the base CMAQ model. A single-day simulation using the CMAQ-Adjoint model, encompassing both forward and backward simulations in our study domain, on average necessitates 2.2×10^5 seconds of CPU time. Extrapolating this to the one-year timeframe of our study, the cumulative CPU time approximates 8.2×10^7 seconds,

translating to roughly 950 days.

We extracted the premature mortalities (i.e., the number of deaths before reaching their life expectancy) from the production sectors related to the food system using the adjoint sensitivities. The premature mortalities specified by production sectors were then linked to the consumption sectors of both rural and urban residents based on the input–output analysis. This process yielded a dataset of $PM_{2.5}$-related health damage for the entire food system, facilitating further analysis of inequality. In contrast to previous methods that directly calculate sector and species contributions using the objective function in the production or emission sector[46-48], our approach establishes a connection between mortality, production, and consumption sectors within the food system based on the consumption-based emission inventory.

Inequality evaluation in premature mortality related to $PM_{2.5}$ exposure

We introduced SDHII to evaluate the inequality in air quality-related health damage attributed to the food system. This index considers the disparity in mortality rates between production- and consumption-based accountings in each province. By population weighting, it quantifies the inequality in mortality rates between production and consumption at the national level. The more intuitive explanation of this index is visualized in Supplementary Fig. 8. The calculation process comprises two steps.

First, we calculated the disparity between premature mortalities attributed to food production (M_P) and consumption (M_C) for each province, which is denoted as ΔM^i and represents the difference in health damage incurred in a region owing to local food production versus the health damage expected from local food consumption within the same region (accounting for local and nonlocal food sources). Mathematically, it is defined by Eq. (11):

$$\Delta M^i = M_P^i - M_C^i \quad (11),$$

where M_P^i and M_C^i represent the M_P rate (deaths per 10,000 population) in the supply side (i.e., province i supplies food to other regions) and the M_C rate (deaths per 10,000 population) in the demand side (i.e., province i receives food from other provinces) for a given province i.

The ΔM rates represent the level of balance between the M_P and M_C rates with the food system. When the mortality rates from regional food production and consumption are balanced, ΔM equals zero. If ΔM^i is >0 for a specific province, it indicates that the region experiences an excess number

of deaths owing to its food supply to other regions. These provinces are referred to as "production-oriented," while provinces with lower health damage ($M_C > M_P$) are labeled as "consumption-oriented."

Next, we ranked all the ΔM rates in ascending order and paired them with population data from each region (Supplementary Fig. 8a), following which the SDHII was computed using Eq. (12):

$$SDHII = \frac{\sum_{i=1}^{n} POP_i \times |M_P^i - M_C^i|}{POP} \quad (12),$$

where POP and POP_i represent the national population and population for a given province i, respectively, and n denotes the total number of provinces.

Intuitively, SDHII corresponds to the area depicted in Supplementary Fig. 8b. This index represents the level of national-scale inequality in health damage. It incorporates population proportion as a weighting factor and captures the regional disparities arising from food production and consumption. When the health damage experienced by a particular region aligns with the expected damage based on food consumption, the ΔM rates for that region are zero, indicating no contribution to SDHII. In an ideal scenario, each region bears health damage proportionate to its consumption, resulting in a balanced distribution of premature mortalities and an SDHII value of 0.

To trace the manifestation of health damages across different income groups, we employed the provincial income data obtained from the National Bureau of Statistics of China[5] to categorize all provinces into ten income groups. Given that the income dataset distinguishes between urban and rural residents for each province, we further classified each province into two population subsets: urban and rural. Consequently, this resulted in a total of 62 distinct population subsets across 31 provinces/regions under consideration. These population subsets were subsequently assigned to ten income groups, with each group comprising six population subsets, except for the lowest income group which comprised ten subsets (Supplementary Table 2). The division of the income groups is illustrated in Supplementary Fig. 27. Next, we conducted pairwise matching among the income groups and calculated the difference in health damage resulting from reciprocal food supply between them, enabling us to evaluate the net premature mortality caused by the intergroup food supply, which is denoted as net ΔM, and can be expressed by:

$$\text{net } \Delta M^{i,j} = \Delta M^{i,j} - \Delta M^{j,i} \quad (13),$$

where net $\Delta M^{i,j}$ represents the net premature mortality between the selected income group i and

another given income group j. This metric evaluates the net health damage between the different income groups after offsetting the respective health damage associated with food consumption. If net $\Delta M^{i,j}$ is >0, the income group j causes excess health damage to the income group i and gains health benefits from food trade owing to the food supply from i to j. Conversely, if net $\Delta M^{i,j}$ is <0, the group j experiences more health damage because of the food supply to the group i.

Intervention strategies

We investigated the potential cobenefits of reducing inequality from various intervention approaches aimed at reducing emission or developing a balanced diet. We designed three intervention scenarios: agricultural emission mitigation, diet transition, and agricultural production reallocation. Each scenario includes several subscenarios that differ in implementation intensity, feasibility, and expected benefits (Table 1).

We conducted six subscenarios to mitigate agricultural NH_3 emissions, comprising four single and two collaborative measures, as outlined by Kang et al.[32] and Adalibieke et al.[19]. The "Intergrated NH_3 reduction strateges" (EM1) scenario involves the incorporation of reduced fertilizer application, deep fertilizer placement, and the use of a urease inhibitor. In the "Increasing mechanized deep fertilization" (EM2) scenario, the incorporation proportion of synthetic N fertilizers is set to reach 80% for wheat, maize, and rice based on the National Agriculture Mechanization Extension Plan[49]. In the "Optimizing fertilizer types" (EM3) scenario, we assumed that 50% of N applications were allocated to organic fertilizer and manure for major crops, vegetables, and fruits[49]. In the "Optimizing fertilzer rates" (EM4) scenario, the N fertilizer rate was reduced to meet the "N Surplus Benchmarks" in seven regions, as proposed by Zhang et al.[50] and the European Union Nitrogen Expert Panel[51]. The regional "N Surplus Benchmarks" were utilized as the targeted N surplus in regions where the N surplus exceeds the benchmarks.

For the diet transition scenario, we explored the potential for reducing inequality by adopting healthier dietary habits. Our dietary recommendations were based on the 2022 Chinese Dietary Guidelines (CDG 2022). The scenario considered nine food categories: grains, vegetables, fruits, pig meat, beef, sheep and goat, poultry, dairy, and eggs. Using CDG 2022 as a reference, we designed four subscenarios for the entire population, balancing healthfulness and feasibility to varying degrees. The four subscenarios included (1) adjusting food intake for each category to the upper limit of the recommended range in CDG (DT1); (2) adjusting food intake for each category to the

lower limit of the recommended range in CDG (DT2); (3) adjusting food intake for each category based on the minimum difference between the existing diet and the recommended range (DT3); and (4) adjusting food intake for each category to the average values of the recommended range in CDG (DT4). For example, if the current food intake exceeded the upper limit of the recommended range, it was adjusted to the upper limit range. Conversely, if the intake was below the lower limit, it was adjusted to the lower limit. No adjustments are made if the current intake is already within the recommended range. We computed the percentage of changes in food intake owing to the dietary transition of each food category, which formed the diet transition matrix (labeled as H_3), based on which we recalculated the premature mortality for each food category in each province to represent the changes in health damage and equality for each subscenario.

Agricultural production reallocation aimed to mitigate health damage by redistributing crop production from high- to low-sensitivity areas. Certain regions are more susceptible to $PM_{2.5}$ emission, leading to more premature deaths per production unit than other regions. Herein, we assumed a fixed spatial distribution of farmlands to avoid potential environmental footprints related to alterations in land use, such as new farmland cultivation[7,52]. Thus, we analyzed crop reallocation by transferring production from farmlands with high $PM_{2.5}$ sensitivity to existing farmlands with $PM_{2.5}$ sensitivity while maintaining crop yield. This transfer of crop yield from high- to low-sensitivity areas requires a certain level of yield increase in those low-sensitivity regions. While concentrating crop production in the areas with the lowest sensitivity would ideally maximize health benefits, it is impractical owing to the limited production potential. We assumed a 30% yield increase in each crop production area and a maximum reduction of 20% in the total crop production in high-sensitivity areas considering the yield ceiling in low-sensitivity areas. Consequently, we designed 20 subscenarios to transfer production from regions with higher mortality rates per unit production (1%–20% of the total production) to regions with lower mortality rates. First, we calculated the mortality rate per unit of crop production for each province using data from the Chinese National Bureau of Statistics[5]. Then, starting with the province with the highest mortality rates (province A), we transferred crop yield to the province with the lowest mortality rates (province B) until the yield increase in province B reached 30% of its initial crop yield. This process was repeated for the second-best province and continued until the total transferred production yield reached 20%. We achieved the desired reallocation by sequentially

allocating transferred yields to regions with the lowest mortality rates per unit.

We conducted an assessment of uncertainty and analyzed limitations for our study. Refer to the Supplementary Information for details.

Data availability

The data supporting the findings of this study are available within the article and Supplementary Information. Population, residents' disposable income, and food intake data at the site scale from the National Bureau of Statistics of China are available at http://data.stats.gov.cn/. China Multi-Regional Input–Output Table is available at http://www.ceads.net/data/input_output_tables/. Livestock feeding data is derived from https://www.fao.org/faostat/. Source data for premature mortalities is accessible on Zenodo: https://doi.org/10.5281/zenodo.10645774.

Code availability

Python 3.8 was used for developing the Environmental Extended Input–Output Analysis (EEIOA) and for data analysis. The source codes utilized in this study can be accessed on Zenodo: https://doi.org/10.5281/zenodo.10645774.

Acknowledgements

G.S. and H.S. acknowledge funding from Ministry of Science and Technology of the People's Republic of China (2023YFE0112900). H.S. acknowledges funding from the National Natural Science Foundation of China (42192510). F.Z. acknowledges funding from the National Natural Science Foundation of China (42225102). S.T. acknowledges funding from the National Natural Science Foundation of China (41991312, 41821005, and 41830641). T.-M.F. and H.S. acknowledge funding from Shenzhen Science and Technology Program (JCYJ20220818100611024). G.S. acknowledges funding from the National Natural Science Foundation of China (42077328). X.Y., T.-M.F., and H.S. acknowledge funding from the Shenzhen Key Laboratory of Precision Measurement and Early Warning Technology for Urban Environmental Health Risks (ZDSYS20220606100604008), Department of Science and Technology of Guangdong Province (2021B1212050024), and Department of Education of Guangdong Province (2021KCXTD004). H.S. acknowledges support

from Center for Computational Science and Engineering at Southern University of Science and Technology.

Author contributions

H.S., J.M., P.H., and F.Z. conceived and initiated the study. L.Z. and W.A. processed and analyzed the data. Y.C., P.G., J.H., and Y.Z. provided support with data collection and processing. P.X., C.W., J.Y., and L.Z. assisted in the development of the model framework. L.Z. drafted the manuscript, and G.S., T.-M. F., and X.Y. participated in the result discussions. H.S., F.Z., J.M., P.H., S.Z., A.H., S.T., and A.G.R. provided critical revisions.

Competing interests

The authors declare no competing interests.

Tables

Table 1 | Description of designed scenarios. EM1 is developed by Kang et al.[32], which incorporates the implementation of reduced fertilizer application, deep fertilizer placement as well as the use of a urease inhibitor; EM2–6 are developed by Adalibieke et al.[19].

Scenario	Sub-scenario	Description
BAU		Business-as-usual
Emission mitigation	EM1	Intergrated NH_3 reduction strateges
	EM2	Increasing mechanized deep fertilization
	EM3	Optimizing fertilizer types
	EM4	Optimizing fertilzer rates
	EM5	Integrating EM2 and EM3
	EM6	Integrating EM2, EM3 and EM4
Diet transition	DT1	Adhering to the maximum recommended food intake in the 2022 Chinese Dietary Guidelines (CDG)
	DT2	Adhering to the minimum recommended food intake in the 2022 CDG
	DT3	Minimum adjustments to resident's diet based on the 2022 CDG
	DT4	Adhering to the average recommended food intake in the 2022

Figure Captions

Fig. 1 | Provincial-level distributions and inequalities of premature mortalities due to food production and consumption in China. Annual premature mortality rates from (**a**) food production (M_P rates) and (**b**) food consumption (M_C rates). (**c**) Difference between M_P rates and M_C rates (ΔM rate). (**d**) The Gini coefficients of M_P rates and M_C rates. The provincial boundary shapefile has been obtained from Harvard Dataverse (https://doi.org/10.7910/DVN/DBJ3BX) and is publicly available under the Creative Commons CC0 Public Domain Dedication.

Fig. 2 | Inequality within the food system across food types. Shown are ΔM rates (difference in mortality rates attributable to $PM_{2.5}$ exposure from food production versus consumption) of each province, sorted in ascending order. The provinces with ΔM mortality rates >0 (on the right side of the curves) are "production-oriented" provinces, indicating that the mortality from local food production surpass that attributed to food consumption. Conversely, if the ΔM rates are <0 (i.e., "consumption-oriented" provinces), the opposite holds true. The inequalities are quantified as the Supply–Demand Health Inequality Index, indicated in parentheses in the legend for each food type.

Fig. 3 | Mortality disparity across income groups. (**a**) Relationship between income and premature mortality, including premature mortality rates attributed to food production (M_P rates) and consumption (M_C rates). We sorted all provinces based on residents' disposable income and categorized them into ten income groups in descending order (D1–D10; Methods and Data). The shading indicates the range between the 25th and 75th percentiles. (**b**) Mortality rate differences attributable to $PM_{2.5}$ exposure from food production vs. consumption (ΔM per 10,000 population) by income decile. The impacts of various food types on ΔM rates differ among income groups, with each type contributing positively or negatively. The net ΔM rates are presented as black dots.

Fig. 4 | The net gap of premature mortalities between production and consumption (net ΔM) is shown for each pair of income groups. Net ΔM in each cell indicates the gap of premature mortality after deducting the equivalent mortality due to mutual food supply for a given pair of income groups. This result represents the attribution of mortality responsibilities in two specified

regions after considering the balance between production and consumption. All provinces in China were classified into ten income groups based on residents' disposable income in 2017[5], denoted as D1–D10, representing income groups in descending order (i.e., D1 is the highest income group; see Methods and Data). As each region is simultaneously a food supplier and consumer, we defined "R1" and "R2" to establish the direction for statistical and visual purposes. If the number of deaths is positive, the group in "R1" caused a net ΔM toll suffered by "R2," while negative means the opposite. For instance, the positive result in the cell at the intersection of row D7 and column D3 indicates that more health damage is incurred on D7 by D3 in mutual supply. Seven food types were considered, namely, grains, vegetables, fruits, pig meat, beef, sheep and goat, poultry, dairy, and eggs. The overall attribution of net ΔM is visible in (**a**), while the details for different food types are presented in (**b**).

Fig. 5 | The changes in the food system inequality and premature mortalities in response to different intervention strategies. We considered emission mitigation and diet transition here. Each scenario includes specific sub scenarios to reflect the impacts of different intervention intensities on inequality, which are pairwise to present the results of combined measures (Table 1). Scenarios solely considering the production-side (excluding diet transition) are represented on the column for "BAU." Meanwhile, scenarios considering only diet transition are represented on the row for "BAU." Inequality is represented using the SDHII, indicated by color in the graph, while premature mortalities is represented by the size of bubbles. The bubble in the bottom left corner corresponds to the business-as-usual scenario, where no adjustments are made to both production- and consumption-side.

References

1. Rudel, T. K. et al. Agricultural intensification and changes in cultivated areas, 1970–2005. *Proceedings of the National Academy of Sciences* **106**, 20675-20680 (2009).
2. Bentham, J. *et al.* Multidimensional characterization of global food supply from 1961 to 2013. *Nature Food* **1**, 70-75 (2020).
3. Kinnunen, P. et al. Local food crop production can fulfil demand for less than one-third of the population. *Nature Food* **1**, 229-237 (2020).
4. Huang, X. et al. A high‐resolution ammonia emission inventory in China. *Global Biogeochemical Cycles* **26** (2012).
5. NBS. *China Statistical Yearbook* 2017 (China Statistics Press, 2018).
6. Tessum, C. W. et al. Inequity in consumption of goods and services adds to racial–ethnic disparities in air pollution exposure. *Proceedings of the National Academy of Sciences* **116**, 6001-6006 (2019).
7. Foley, J. A. et al. Solutions for a cultivated planet. *Nature* **478**, 337-342 (2011).
8. Chen, X. et al. Producing more grain with lower environmental costs. *Nature* **514**, 486-489 (2014).
9. Springmann, M. *et al.* Options for keeping the food system within environmental limits. *Nature* **562**, 519-525 (2018).
10. Gu, B. et al. Cost-effective mitigation of nitrogen pollution from global croplands. *Nature* **613**, 77-84 (2023).
11. Godfray, H. C. J. et al. Meat consumption, health, and the environment. *Science* **361**, eaam5324 (2018).
12. Poore, J. & Nemecek, T. Reducing food's environmental impacts through producers and consumers. *Science* **360**, 987-992 (2018).
13. Hasegawa, T., Havlík, P., Frank, S., Palazzo, A. & Valin, H. Tackling food consumption inequality to fight hunger without pressuring the environment. *Nature Sustainability* **2**, 826-833 (2019).
14. Clark, M. et al. Estimating the environmental impacts of 57,000 food products. *Proceedings of the National Academy of Sciences* **119**, e2120584119 (2022).
15. Halpern, B. S. et al. The environmental footprint of global food production. *Nature Sustainability* **5**, 1027-1039 (2022).
16. Carter, C. A. China's agriculture: Achievements and challenges. ARE Update 14, 5-7 (2011).
17. Lam, H.-M., Remais, J., Fung, M.-C., Xu, L. & Sun, S. S.-M. Food supply and food safety issues in China. *The Lancet* **381**, 2044-2053 (2013).
18. He, P., Baiocchi, G., Hubacek, K., Feng, K. & Yu, Y. The environmental impacts of rapidly changing diets and their nutritional quality in China. *Nature Sustainability* **1**, 122-127 (2018).
19. Adalibieke, W. et al. Decoupling between ammonia emission and crop production in China due to policy interventions. *Global Change Biology* **27**, 5877-5888 (2021).
20. Wang, C. et al. A high-resolution ammonia emission inventory for cropland and livestock production in China. *Chinese Journal of Eco-Agriculture* **29**, 1973−1980 (2021).
21. Meng, W. *et al.* Improvement of a global high-resolution ammonia emission inventory for combustion and industrial sources with new data from the residential and transportation sectors. *Environmental science & technology* **51**, 2821-2829 (2017).
22. Huang, Y. *et al.* Quantification of global primary emissions of $PM_{2.5}$, PM_{10}, and TSP from combustion and industrial process sources. *Environmental science & technology* **48**, 13834-13843 (2014).
23. Huang, T. *et al.* Spatial and temporal trends in global emissions of nitrogen oxides from 1960 to 2014. *Environmental science & technology* **51**, 7992-8000 (2017).

24. Huang, Y. *et al.* Global organic carbon emissions from primary sources from 1960 to 2009. *Atmospheric Environment* **122**, 505-512 (2015).
25. Xu, H. *et al.* Updated global black carbon emissions from 1960 to 2017: improvements, trends, and drivers. *Environmental Science & Technology* **55**, 7869-7879 (2021).
26. Zhao, S. et al. A multiphase CMAQ version 5.0 adjoint. *Geoscientific Model Development* **13**, 2925-2944 (2020).
27. Sans, P. & Combris, P. World meat consumption patterns: An overview of the last fifty years (1961–2011). *Meat Science* **109**, 106-111 (2015).
28. Bell, W., Lividini, K. & Masters, W. A. Global dietary convergence from 1970 to 2010 altered inequality in agriculture, nutrition and health. *Nature Food* **2**, 156-165 (2021).
29. Ma, L., Long, H., Tu, S., Zhang, Y. & Zheng, Y. Farmland transition in China and its policy implications. *Land Use Policy* **92**, 104470 (2020).
30. Xue, L. et al. China's food loss and waste embodies increasing environmental impacts. *Nature Food* **2**, 519-528 (2021).
31. Maclean, W. et al. Food energy—methods of analysis and conversion factors. *Food and agriculture organization of the united nations technical workshop report* (2003).
32. Kang, J. et al. Ammonia mitigation campaign with smallholder farmers improves air quality while ensuring high cereal production. *Nature Food*, 1-11 (2023).
33. Institute for Health Metrics and Evaluation (IHME), *The Cost of Air Pollution: Strengthening the Economic Case for Action*; 2016. http://hdl.handle.net/10986/25013.
34. *UN Sustainable Development Goals. Goal 10: Reduce inequality within and among countries*. (UN Sustainable development group, 2022); https://www.un.org/sustainabledevelopment/inequality/
35. Zhai, F. et al. Prospective study on nutrition transition in China. *Nutrition reviews* **67**, S56-S61 (2009).
36. Xu, W. et al. Increasing importance of ammonia emission abatement in $PM_{2.5}$ pollution control. *Science Bulletin* (2022).
37. Chen, Y., Shen, H. & Russell, A. G. Current and future responses of aerosol pH and composition in the US to declining SO_2 emissions and increasing NH_3 emissions. *Environmental Science & Technology* **53**, 9646-9655 (2019).
38. Zheng, H. et al. Chinese provincial multi-regional input-output database for 2012, 2015, and 2017. *Scientific Data* **8**, 244 (2021).
39. Burnett, R. et al. Global estimates of mortality associated with long-term exposure to outdoor fine particulate matter. *Proceedings of the National Academy of Sciences* **115**, 9592-9597 (2018).
40. *FAOSTAT: FAO Statistical Databases*. http://www.fao.org/faostat/en/ (Food and Agriculture Organization of the United Nations, 2017).
41. Liu, X. et al. Dietary shifts can reduce premature deaths related to particulate matter pollution in China. *Nature Food* **2**, 997-1004 (2021).
42. NBS. *China energy statistical yearbook 2017*. (China Statistics Press, 2017).
43. Zhao, H. et al. Assessment of China's virtual air pollution transport embodied in trade by using a consumption-based emission inventory. *Atmospheric Chemistry and Physics* **15**, 5443-5456 (2015).
44. Shen, H. et al. Novel method for ozone isopleth construction and diagnosis for the ozone control strategy of Chinese cities. *Environmental Science & Technology* **55**, 15625-15636 (2021).
45. Zhou, M. et al. Mortality, morbidity, and risk factors in China and its provinces, 1990–2017: a systematic analysis for the Global Burden of Disease Study 2017. *The Lancet* **394**, 1145-1158 (2019).
46. Wang, X. et al. Sensitivities of ozone air pollution in the Beijing–Tianjin–Hebei area to local and

upwind precursor emissions using adjoint modeling. *Environmental Science & Technology* **55**, 5752-5762 (2021).

47. Pappin, A. J. & Hakami, A. Source attribution of health benefits from air pollution abatement in Canada and the United States: an adjoint sensitivity analysis. *Environmental Health Perspectives* **121**, 572-579 (2013).
48. Wang, M., Yim, S. H., Dong, G., Ho, K. & Wong, D. Mapping ozone source-receptor relationship and apportioning the health impact in the Pearl River Delta region using adjoint sensitivity analysis. *Atmospheric Environment* **222**, 117026 (2020).
49. Zhang, X. et al. Societal benefits of halving agricultural ammonia emissions in China far exceed the abatement costs. *Nature Communications* **11**, 4357 (2020).
50. Zhang, C., Ju, X., Powlson, D., Oenema, O. & Smith, P. Nitrogen surplus benchmarks for controlling N pollution in the main cropping systems of China. *Environmental Science & Technology* **53**, 6678-6687 (2019).
51. Panel, E. N. E. Nitrogen use efficiency (NUE): an indicator for the utilization of nitrogen in food systems. *Wageningen University, Alterra, Wageningen, Netherlands* (2015).
52. Hong, C. et al. Global and regional drivers of land-use emissions in 1961–2017. *Nature* **589**, 554-561 (2021).

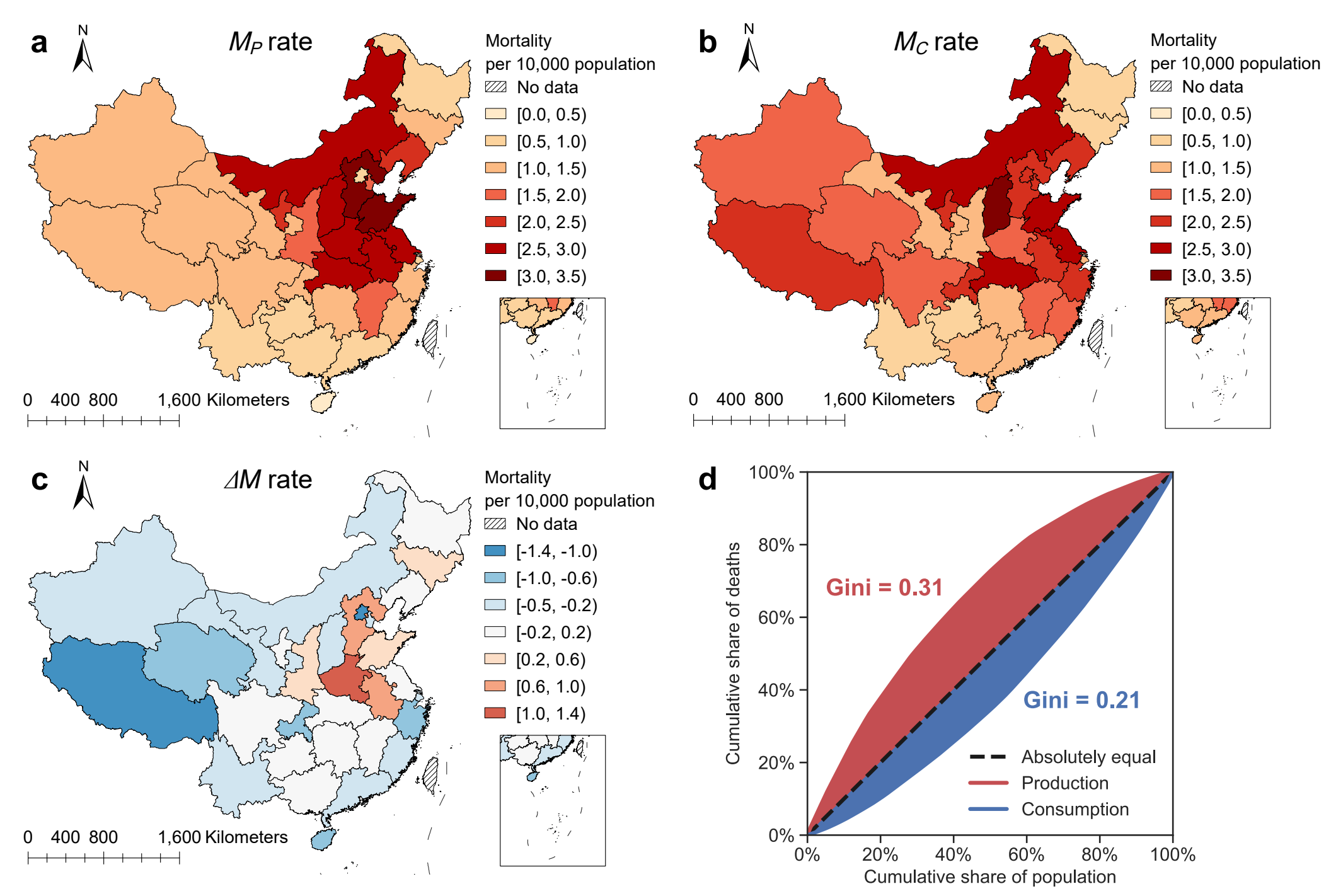
a
N
M_P rate
Mortality
per 10,000 population
No data
[0.0, 0.5)
[0.5, 1.0)
[1.0, 1.5)
[1.5, 2.0)
[2.0, 2.5)
[2.5, 3.0)
[3.0, 3.5)
0 400 800 1,600 Kilometers
b
N
M_C rate
Mortality
per 10,000 population
No data
[0.0, 0.5)
[0.5, 1.0)
[1.0, 1.5)
[1.5, 2.0)
[2.0, 2.5)
[2.5, 3.0)
[3.0, 3.5)
0 400 800 1,600 Kilometers
c
N
ΔM rate
Mortality
per 10,000 population
No data
[-1.4, -1.0)
[-1.0, -0.6)
[-0.5, -0.2)
[-0.2, 0.2)
[0.2, 0.6)
[0.6, 1.0)
[1.0, 1.4)
0 400 800 1,600 Kilometers
d
Cumulative share of deaths
100%
80%
60%
40%
20%
0%
Gini = 0.31
Gini = 0.21
Absolutely equal
Production
Consumption
0% 20% 40% 60% 80% 100%
Cumulative share of population

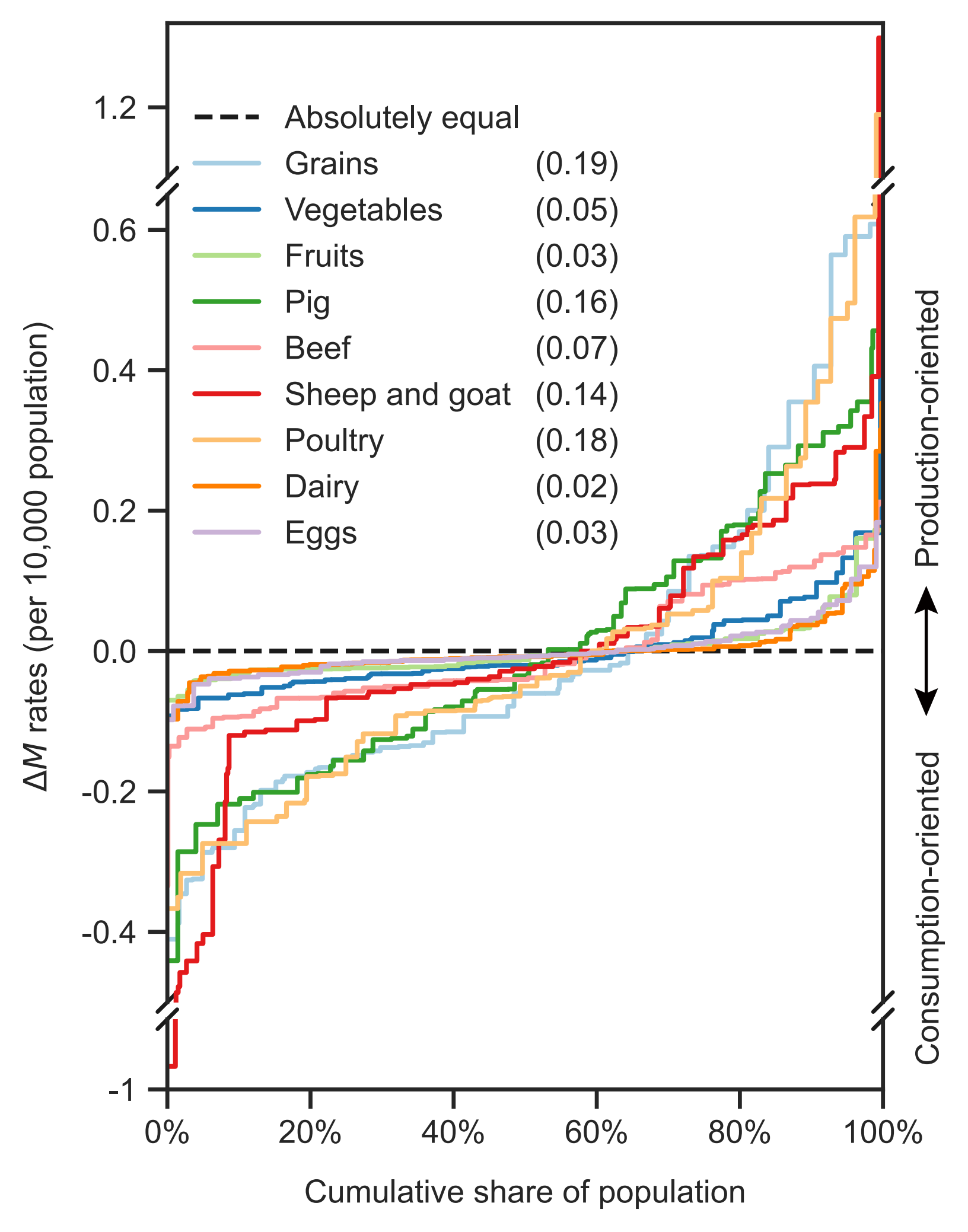
Absolutely equal
Grains (0.19)
Vegetables (0.05)
Fruits (0.03)
Pig (0.16)
Beef (0.07)
Sheep and goat (0.14)
Poultry (0.18)
Dairy (0.02)
Eggs (0.03)
1.2
0.6
0.4
0.2
0.0
-0.2
-0.4
-1
ΔM rates (per 10,000 population)
Production-oriented
Consumption-oriented
0%
20%
40%
60%
80%
100%
Cumulative share of population

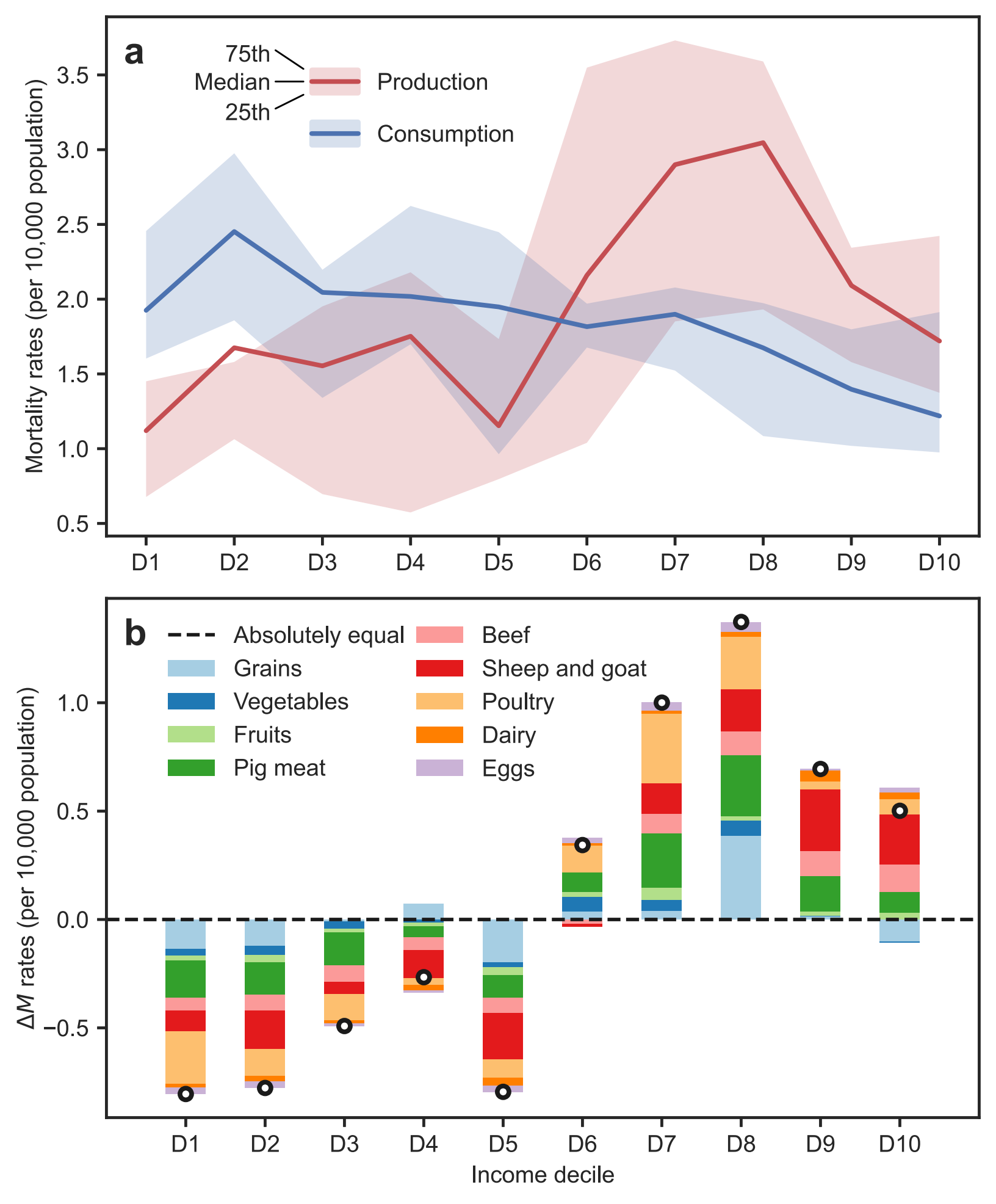
a
75th
Median
25th
Production
Consumption
Mortality rates (per 10,000 population)
3.5
3.0
2.5
2.0
1.5
1.0
0.5
D1
D2
D3
D4
D5
D6
D7
D8
D9
D10
b
Absolutely equal
Grains
Vegetables
Fruits
Pig meat
Beef
Sheep and goat
Poultry
Dairy
Eggs
ΔM rates (per 10,000 population)
1.0
0.5
0.0
−0.5
D1
D2
D3
D4
D5
D6
D7
D8
D9
D10
Income decile

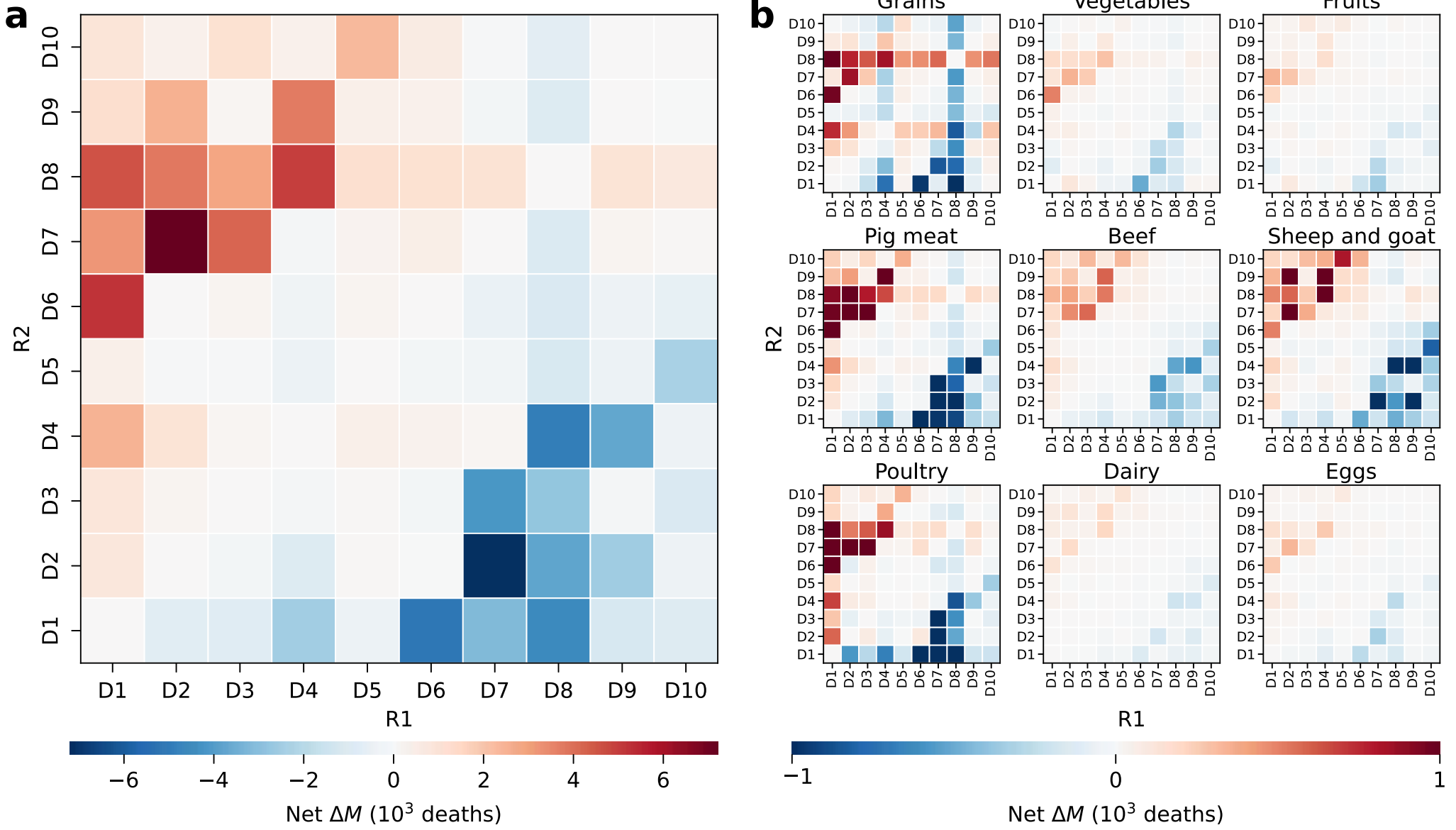
a
b
R1
R2
D1
D2
D3
D4
D5
D6
D7
D8
D9
D10
Net ΔM (10^3 deaths)
−6
−4
−2
0
2
4
6
Grains
Vegetables
Fruits
Pig meat
Beef
Sheep and goat
Poultry
Dairy
Eggs
−1
0
1

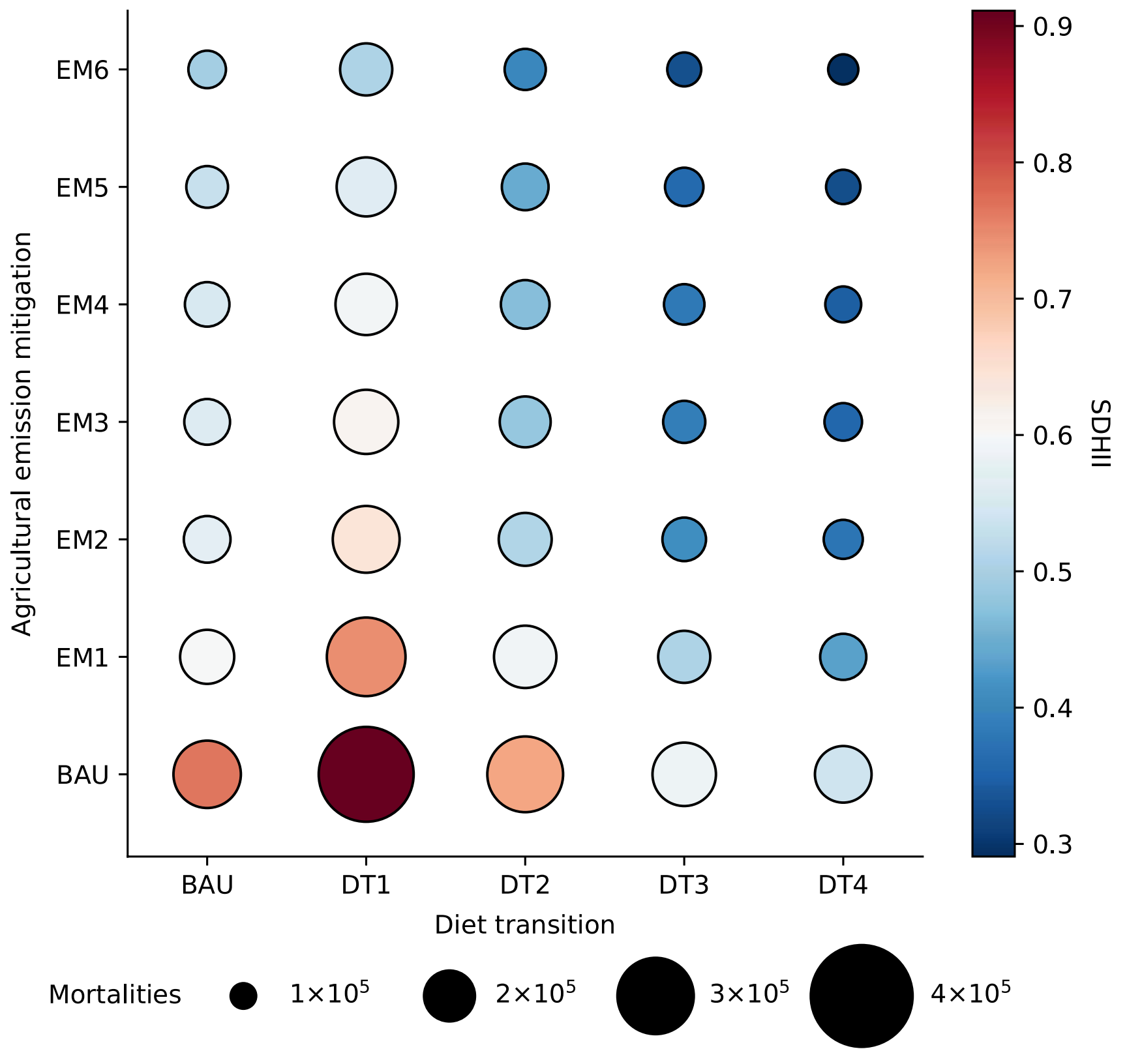
EM6
EM5
EM4
EM3
EM2
EM1
BAU
Agricultural emission mitigation
BAU
DT1
DT2
DT3
DT4
Diet transition
SDHII
0.9
0.8
0.7
0.6
0.5
0.4
0.3
Mortalities
1×10^5
2×10^5
3×10^5
4×10^5